GENERIC MULTIVARIATE MODEL FOR COLOR TEXTURE CLASSIFICATION IN RGB COLOR SPACE

Ahmed Drissi El Maliani, Mohammed El Hassouni, Yannick Berthoumieu, Driss Aboutajdine

Noname manuscript No.
(will be inserted by the editor)

GENERIC MULTIVARIATE MODEL FOR COLOR TEXTURE CLASSIFICATION IN RGB COLOR SPACE

Ahmed Drissi El Maliani · Mohammed El Hassouni · Yannick Berthoumieu · Driss Aboutajdine

Received: date / Accepted: date

Abstract This paper presents a new method for modeling magnitudes of dual tree complex wavelet coefficients, in the context of color texture classification. Based on the characterization of dependency between RGB color components, Gaussian copula associated with Generalized Gamma marginal function is proposed to design the multivariate generalized Gamma density (MGΓD) modeling. MGΓD has the advantages of genericity in terms of fitting over a variety of existing joint models. On the one hand, the generalized Gamma density function offers free-shape parameters to characterize a wide range of heavy-tailed densities, i.e. the genericity. On the other hand, the inter-component,inter-band dependency is captured by the Gaussian Copula which offers adapted flexibility. Moreover, this model leads to a closed-form for the probabilistic similarity measure in terms of parameters, i.e. Kullback Leibler divergence. By exploiting the separability between the copula and the marginal spaces, the closed-form enables us to minimize the computational time needed to measure the discrepancy between two Multivariate Generalized Gamma densities in comparison to other models which imply of using a Monte-Carlo method characterized by an expensive time-computing. For evaluating the performance of our proposal, a K-Nearest Neighbor (KNN) classifier is then used

F. Author
LRIT, Unité Associée au CNRST (URAC 29), Université Mohammed V, Agdal, Morocco
E-mail: meliani.ahmed@hotmail.fr

S. Author
DESTEC, FLSHR, Université Mohammed V, Agdal, Morocco
E-mail: mohamed.elhassouni@gmail.com

T. Author
Univ. Bordeaux, IPB, IMS, Groupe Signal, UMR 5218, F-33400 Talence, France
E-mail: yannick.berthoumieu@ims-bordeaux.fr

T. Author
LRIT, Unité Associée au CNRST (URAC 29), Université Mohammed V, Agdal, Morocco
E-mail: aboutaj@fsr.ac.ma

to test the classification accuracy. Experiments on different benchmarks using color texture databases are conducted to highlight the effectiveness of the proposed model associated to the Kullback-Leibler divergence.

Keywords Classification · Texture · Copula · Kullback-Leibler divergence

1 Introduction

For various practical applications in computer vision, texture analysis is a useful and key component for solving problems such as pattern recognition, classification or segmentation. Thus, in practical applications, an efficient modeling of the variation of intensity that characterizes the texture in the image is central. The relevance of the model determines to a large extent the effectiveness of the feature extraction and then the performance of the image processing method. However, as relevant as the model is, it is also important to propose an appropriate similarity measure and easy to use.
Many recent works devoted to texture stressed that accurate feature extraction can be achieved by statistical modeling of subband coefficients in the transformed domain of wavelets. A variety of wavelet decompositions can be applied, ranging from Discret Wavelet Transform (DWT), Steerable Pyramids, to the recent complex wavelet transforms [6]. Each of these transformations has some particularities, but all share the property sparsity of their subband distributions. Histograms are heavy tailed and pickily pronounced, and then need to a sub-Gaussian modeling. To fulfill this need, a pioneering work where Do and Vetterli proposed the Generalized Gaussian Density (GGD)[1] as an alternative to the Gaussian model. Recently, the magnitudes of complex subbands coefficients have been modeled by Weibull and Gamma distributions [2] [3], leading to a considerable enhancement of the retrieval performances. In the same way, we have proposed the Generalized Gamma distribution as a model for the coefficient magnitudes issued from the Dual Tree Complex Wavelet Transform (DTCWT), for grey level texture classification issue [9]. A more general work was done inspired by the Generalized Gamma density, but in the context of texture retrieval [10].
In these previous works, only marginal distributions of subband histograms are taken into account. This is suitable for grey level images when independence between subbands of the same scale is supposed. However in the case of color textures, the dependence between color components is undeniable and must be taken into account by conceiving multivariate models, otherwise the system will suffer from the lack of this crucial information. The joint statistical modeling is then a welcome advantage for color texture retrieval or classification. Such framework has been considered previously by many authors. Verdoolaege et al. [5], proposed a multivariate Generalized Gaussian distribution (MGGD) for multiscale color texture retrieval. The model was devoted to describe dependence across color components while assuming independence among subbands of a single color component. In [7][31], Kwitt et al. treated

the problem of joint modeling of complex coefficient magnitudes across subbands of different color components. Based on Gaussian copula and student t copula for modeling the dependence structure, in conjunction with Weibull and Gamma densities as parametric margin models, they achieved significant enhancements in the context of texture retrieval. Another Copula based multivariate modeling was proposed by Sakji-Nsibi et al. [8], for multicomponent image indexing using Gaussian Copula in conjunction with the GGD and Gamma densities. Again substantial improvement of classification results was obtained in comparison with the marginal modeling approach. However, texture databases are extremely increasing in term of diversity and heterogeneity of textures, which limits the use of one model over others. Moreover, the lack of analytical expression for the KL divergence in the case of multivariate models based on copulas presents a shortcoming, since the alternative Monte-Carlo based approach [7][8] is computationally expensive.

Based on these observations and to remedy the problem of complex nature and huge variety of textures in the databases, we propose a generic multivariate model that takes into account the strong dependency between RGB color components. In order to manage the diversity, the Generalized Gamma density is proposed associated to the Gaussian copula for capturing the dependence accross color component subbands of a fixed and/or different pair of orientation at a fixed scale of decomposition, i.e the MGΓD model. The choice of the Multivariate Generalized Gamma based on the Gaussian copula is justified by the existence of KL divergence for Gaussian copula and Generalized Gamma margin model, since we present a closed form of the KL divergence based similarity measure.

Then, contribution in this work is threefold:

- First, concerning the dataset we consider an inter-band inter-component dependency which seems to provide a rich information for the characterization process.
- Second, concerning the model we present MGΓD as a generic multivariate model in order to capture the rich information of dependency between R, G and B components subbands.
- Three, concerning the similarity measurement which is a bit hard to calculate in case of copulas based models. We present a closed form expression of the KL divergence between two MGΓD densities which gives a big advantage over the Monte-carlo based approach.

Experiments using the K-nearest neighbor classifier show the superiority of the Multivariate Generalized Gamma model over the existing joint models, and highlight also the effectiveness of the proposed metric when compared with the Monte-Carlo based approach.

This paper is organized as follows. In the next section, we give an overview of the multivariate statistical modeling in the RGB color space, we present the multivariate proposed model and we derive the Kullback-Leibler divergence. In section 3, we provide texture classification results. Finally, we conclude in the section 4.

2 Multivariate Statistical Modeling in the RGB color space

2.1 Wavelet Domain

For texture analysis, wavelet transform presents advantages in terms of locality, sparsity and spatial-frequency characterization. Thus, this analysis tool received a lot of attention and achieved notoriety in the last decades. In this context, the classical Discret Wavelet Transform (DWT), provides an intuitive description and a non-redundant representation of images. However, the decomposition of an image with a DWT leads to only four directional frequency subbands at each decomposition scale, one is an approximation subband and three are detail subbands corresponding to the vertical, horizontal and diagonal orientations. In addition to this lack of directionality, DWT is not shift invariant, thus each small shifting of the image leads to a significant difference of the wavelet coefficient magnitude for the same subband. The main reason of this problem is the real valued nature of the coefficients of DWT, since that the Fourier transform does not suffer from this one. As an alternative, N. Kingsbury [6] proposed the Dual-Tree Complex Wavelet Transform (DTCWT). The basic idea of this approach consists in using two real wavelets to obtain complex wavelet coefficients, which are shift-invariant. DTCWT provides six detail subbands per scale instead of three subbands in the case of DWT, which presents a rich directional selectivity.
Since we are dealing with color textures in the RGB color space, from each image from the database, color components R, G and B are decomposed via the DTCWT. Let $r_{os} = |R_{s,o}|$, $g_{os} = |G_{s,o}|$, $b_{os} = |B_{s,o}|$, be the subbands representing magnitudes of the coefficients at a fixed scale s and an orientation o. In the next subsection, we investigate the existence of dependencies among coefficients of these subbands.

2.2 Dependency observations

As already mentioned, many works are based on marginal modeling of textures, without accounting for the information that resides across the color components. This approach has the advantage to be simple and tractable, but leads to a considerable loss of the dependence information. Let us scroll some proofs of the nonzero dependence between components, when color textures are represented in the RGB color space. In the following paragraph, some experiments are conducted for some samples of textures from the Vistex database to exhibit the effective dependency between color components in the RGB color space.

2.2.1 Perceptual report

Before providing objective proofs of dependence such as mutual information and scatter plots, one can make a perceptual report even being a subjective

Fig. 1 Color texture Fabric.0015.

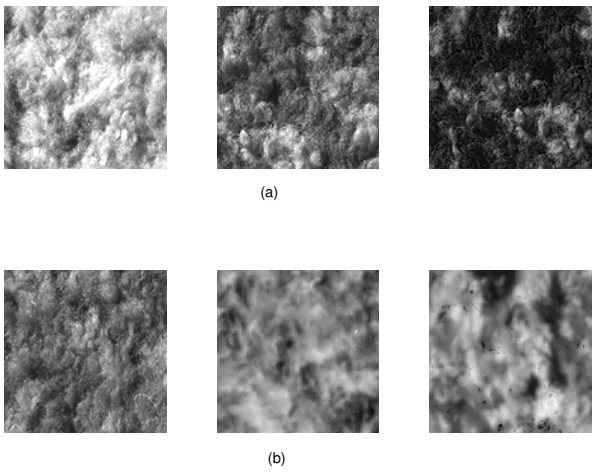

Fig. 2 Spatial structure of color components for texture Fabric.0015 on RGB and Yuv color spaces. (a) R, G and B spatial structures. (b) Y, u and v spatial structures.

one.
The dependence across RGB color components can be observed perceptually, from the texture presented in Fig.1. Clearly observed from Fig.2, the spatial structures of color components of the *Fabric.0015* color texture are extremely close in case of RGB representation (Fig.2(a)), while we observe that in the case of Yuv representation (Fig.2(b)), the spatial structure of the Y component is different compared to spatial structures of u and v components.

2.2.2 Mutual information

Mutual information is a measure of the statistical dependence between two variables. Let X and Y be two random variables, $f(x)$ and $f(y)$ the marginal probability distribution functions of X and Y respectively, and $f(x, y)$ the

joint probability distribution function of X and Y. The mutual information between X and Y is then:

$$I(X,Y) = \sum_{x,y} f(x,y) log \frac{f(x,y)}{f(x)f(y)}$$

X and Y are independent if $I(X,Y) = 0$. Table 1 shows the mutual information

	{R} vs {G}	**{R} vs {B}**	**{G} vs {B}**
Bark.0000	7.72	7.57	7.59
Brick.0000	6.13	5.88	5.82
Fabric.0000	6.19	5.72	5.85
Clouds.0000	6.14	5.62	5.46

Table 1 Mutual information between R, G and B color components.

between R, G and B color components for different color textures from Vistex database [22]. It can be seen that a considerable dependence exists between those components.

2.2.3 Scatter plot test

Scatter plot is a graphical test for assessing dependence between variables. More the points cluster in a band from lower left to upper right, higher the degree of dependence between these variables is.
Fig. 3 shows the scatter plots between color component detail subbands for second scale decomposition. The coefficients presented on Fig. 3 are the Pearson (r), Kendall (ρ) and Spearman (τ) correlation coefficients.
Three kinds of dependence between R, G and B component subbands are presented, namely the inter-component only dependence ((a) and (b)), the {inter-component, inter-band} dependence ((c)), and the inter-band only dependence ((d)). In (a) and (b), we observe a huge dependence between R_o, G_o and bB_o subbands as illustrated by the Pearson coefficient ($r = 0.98$ for $\{R_6$ vs $G_6\}$ and $r = 0.95$ for $\{R_1$ vs $B_1\}$).
In (c) and (d), we measure the degree of dependence, when considering also the inter-band dependence, i.e the dependence between component subbands in different orientations ($\{R_o$ vs $G_{o'}\}$). Here, the scatter plots show that the degree of dependence is considerable ($r = 0.82$ for $\{R_3$ vs $G_4\}$) even it is less than the inter-component one.

2.3 The dataset

In order to improve the characterization, we wish to exploit both inter-component and inter-band dependencies. Thus, the dataset considered for our model is represented by the vector $x_s = [r_{os} \quad g_{os} \quad b_{os}]$, where $o = \{1, ..., N\}$, and N

represents the number of orientations.
Since we use the DTCWT as a wavelet decomposition (with 6 orientations per scale), we may have a dataset with 3×6 columns such as

$$x_s = [r_{1s} \ ... \ r_{6s} \ g_{1s} \ ... \ g_{6s} \ b_{1s} \ ... \ b_{6s}] \quad .$$

Then, in our case, the dependence structure is represented by one 18-by-18 correlation matrix.

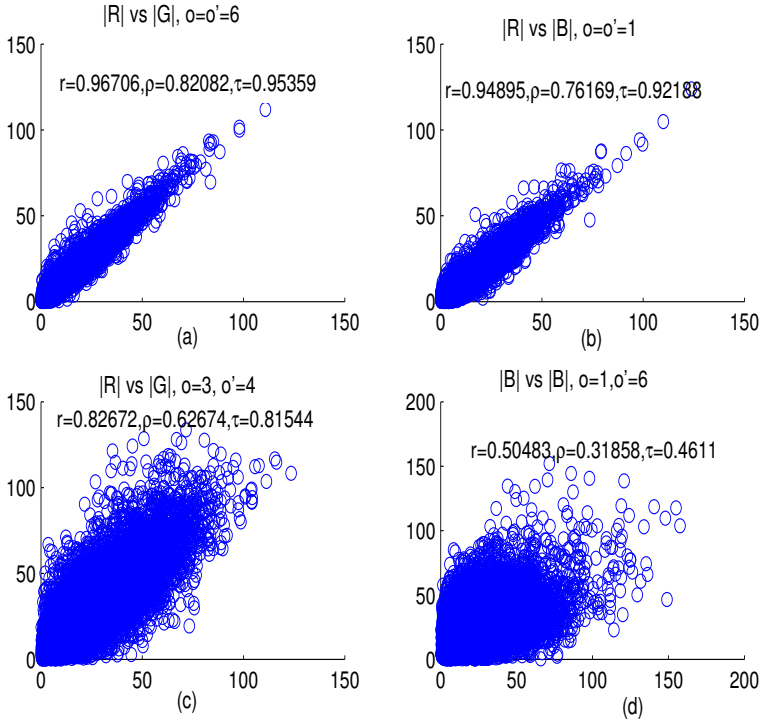

Fig. 3 Scatter plots for different combinations of subbands. (a) and (b) show scatter plots of different color component subbands in a same orientation o (inter-component only dependence). (c) shows scatter plot of different color component subbands in different orientations (inter-component,inter-band dependence). (d) shows scatter plot of different subbands of the same color component (inter-band only dependence).

3 Multivariate Generalized Gamma distribution (MGΓD)

As said in the introduction, our aim is to propose a generic and flexible joint model allowing us to characterize respectively the heavy-tailed behavior and

the information of dependence between color components. We propose the Multivariate Generalized Gamma distribution (MGΓD), drawing on the copula theory. Let us first give a brief review of what are copulas.

3.1 Review of the copula theory

Copulas are a mathematical tool for merging a set of marginal probability density functions (pdfs) into a multivariate pdf with a particular dependence structure. A copula is a multivariate cumulative distribution function defined on the d-dimensional unite cube $[0,1]^d$ [15], with uniform one dimensional marginals. Given a d-dimensional vector $x = (x_1, ..., x_d)$ on the unit cube $[0,1]$, with a joint cumulative distribution function F and marginal cumulative distribution functions (cdf) $F_1, ..., F_d$. The joint cdf is:

$$F(x_1, ..., x_d) = P(X_1 \leq x_1, ..., X_d \leq x_d)) \tag{1}$$

Sklar's theorem [16] shows that there exist a d-dimensional copula C such that:

$$F(x_1, ..., x_d) = C(F_1(x_1), ..., F_d(x_d)) \tag{2}$$

Further, if C is continuous and differentiable, the copula density is given by:

$$c(u_1, ..., u_d) = \frac{\partial^d C(u_1, ..., u_d)}{\partial u_1 ... \partial u_d} \tag{3}$$

The joint pdf is then deduced uniquely from the margins and the copula density as follows:

$$f(x_1, ..., x_d) = c(F_1(x_1), ..., F_d(x_d)) \prod_{i=1}^{d} f_i(x_i) \tag{4}$$

where $f_i, i = 1, ..., d$, represent the marginal densities.
In order to represent structure of dependence, one has in hand different families of copulas such as Archimedian (Fig.4), Gaussian (Fig.5) and t-Student (Fig.6) copulas.

It appears that the Gaussian copula is suitable to model linear dependence which is the most popular in texture modeling and which is the case of the inter-band inter-component we study in this paper. Fig.7 shows that dependence structure for subband coefficients from different components has an elliptical behavior that is well fitted by the Gaussian copula (Fig.5).
The Gaussian copula density is given by:

$$c(u, \Sigma) = \frac{1}{|\Sigma|^{1/2}} \exp[-\frac{1}{2} \vartheta^T (\Sigma^{-1} - I) \vartheta] \tag{5}$$

with $\vartheta_i = \phi^{-1}(F_i(x_i))$, and ϕ represents the standard normal cumulative distribution function. Σ denotes the correlation matrix, and I denotes the d-dimensional identity matrix.

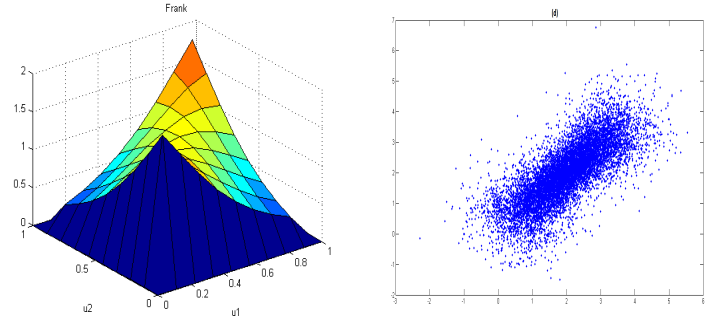

Fig. 4 Left: the Archimedian copula pdf. Right: the structure of dependence generated from an Archimedian copula (with correlation parameter $\rho = 0.1$).

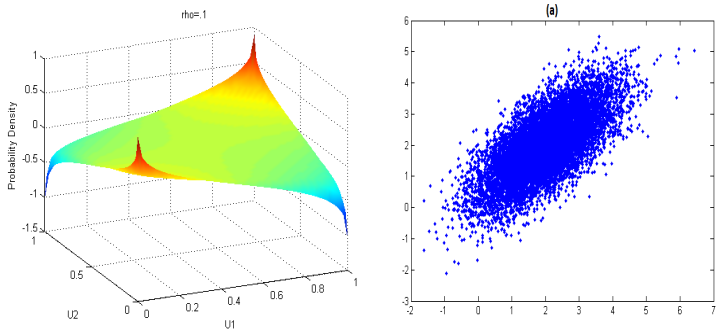

Fig. 5 Left: the Gaussian copula pdf. Right: the structure of dependence generated from a Gaussian copula (with correlation parameter $\rho = 0.1$).

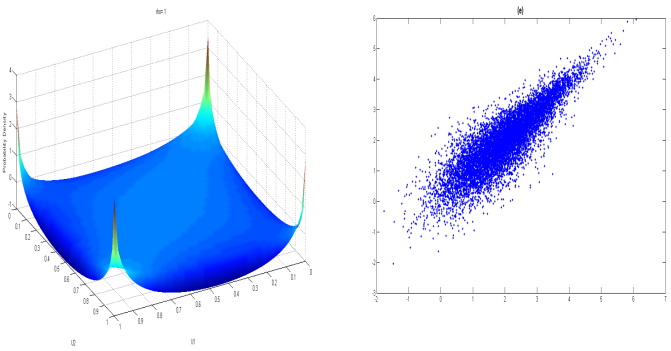

Fig. 6 Left: the t-Student copula pdf. Right: the structure of dependence generated from a t-Student copula (with correlation parameter $\rho = 0.1$).

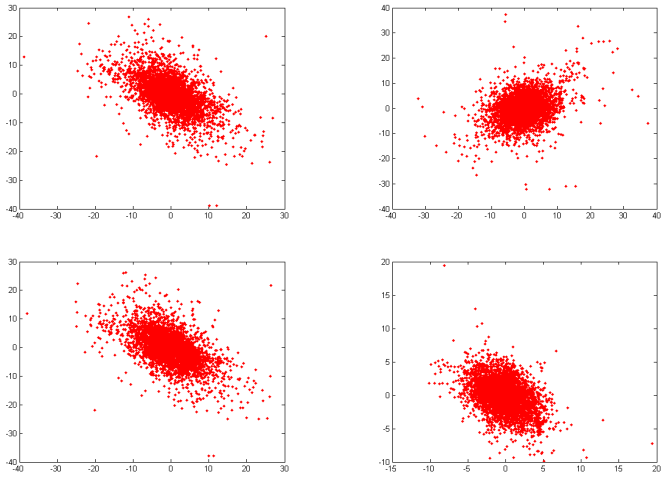

Fig. 7 Structure of inter-component,inter-band dependence between different subbands

3.2 Generalized Gamma distribution

In [9] we used the univariate Generalized Gamma density ($G\Gamma$) in order to fit marginal distributions of the dual tree complex wavelet coefficient magnitudes.

Generalized Gamma was first introduced by Stacy [18] as a generic distribution for modeling duration. In contrast to the Generalized Gaussian Density (GGD), Generalized Gamma has an additional shape parameter, which allows more flexibility in fitting larger classes of subbands histograms. Moreover, the Generalized Gamma provides more genericity since it covers GGD, Weibull, Gamma and a variety of well-known models as special cases. The probability density function of $G\Gamma$ is defined as:

$$f(y;w) = \frac{\tau}{\lambda^{\alpha\tau}\Gamma(\alpha)} y^{\alpha\tau-1} \exp^{-(\frac{y}{\lambda})^{\tau}}, y \geq 0, \alpha, \tau, \lambda > 0 \tag{6}$$

where $w = (\alpha, \tau, \lambda)$ denotes the $G\Gamma$ parameters, α and τ are shape parameters, λ is the scale parameter, and $\Gamma(.)$ is the Gamma function.
From Fig. 8, we can visually conclude that Generalized Gamma model gives a better marginal fitting in comparison with its special cases, i.e Gamma and Weibull densities, considering one subband from a given texture. This behavior remains the same for the whole set of textures within the Vistex database as it is shown in Table 2, where we compute the KL divergence between marginal distributions of textures from the Vistex database and the parametric marginal fitting of our model and its special cases, such as:

$$KL(f_m||f) = \sum_i f_m(i) log \frac{f_m(i)}{f(i)} \tag{7}$$

where f_m represents the empirical marginal probability density function, and f denotes the parametric marginal probability density function (Weibull, Gamma or $G\Gamma$). Results show that $G\Gamma$ model offers the best marginal fitting since it minimizes the KL divergence.

	Bark	**Brick**	**Buildings**	**Flowers**
Weibull	0.23	0.22	0.85	0.33
Gamma	0.12	0.08	0.43	0.19
$G\Gamma$	0.08	0.06	0.35	0.16

Table 2 KLD between the empirical marginal pdf and the parametric ones for several textures.

3.3 The proposed multivariate pdf

Subsections 3.1 and 3.2 showed, respectively, that Gaussian copula is well suited to represent the inter-band inter-component dependency, and that the Generalized Gamma density fits well the marginal behavior of subband coefficients. Based on these conclusions, we repose on a multivariate model which we call Multivariate Generalized Gamma distribution (MGΓD) in order to characterize the joint distribution of color texture subbands (Fig. 9). MGΓD

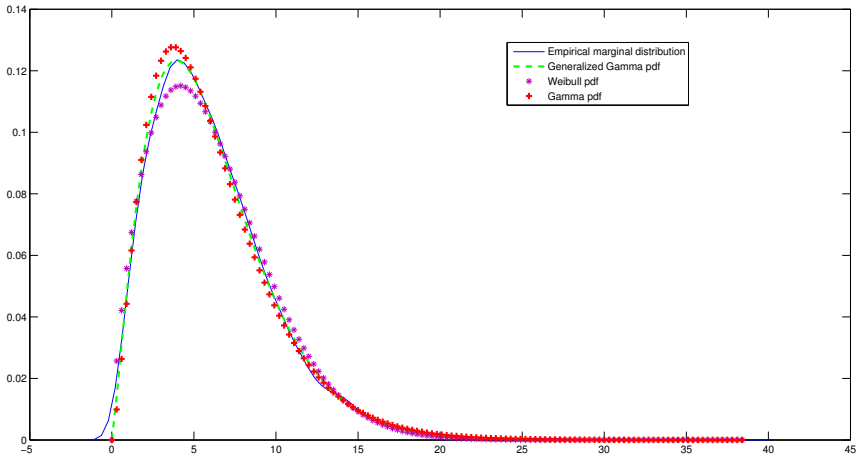

Fig. 8 Marginal fitting for texture 'Fabric.0015' from Vistex database, using different univariate models.

is based on a Gaussian copula in conjunction with the $G\Gamma$ density. Thus, from equations (4) and (6), we derive the (MGΓD) density as:

$$f(x,\theta) = \frac{1}{|\Sigma|^{1/2}} \exp[-\frac{1}{2}\vartheta^T(\Sigma^{-1} - I)\vartheta]\times$$

$$(\frac{\tau}{\lambda^{\alpha\tau}\Gamma(\alpha)})^d \exp[-\sum_{i=1}^{d}(\frac{x_i}{\lambda})^\tau]\prod_{i=1}^{d} x_i^{\alpha\tau-1} \tag{8}$$

where $\theta = (\alpha, \tau, \lambda, \Sigma)$ denotes the hyperparameters of the joint model.
It is worth recalling here that the joint modeling presents big advantages over the marginal modeling in terms of consideration of the dependence information that exists between subband coefficients. Thus, it is natural that MGΓD model is gainful compared to univariate GGD or $G\Gamma$ models for example.
Fig. 10 shows scatter plots of original color subband coefficient magnitudes against samples from a MGΓD modeling after estimating subbands combination between color channels (column 1), along with the joint fitting of the MGΓD model on the empirical joint distributions of subband coefficients (column 2). We observe that the model fits very well the combination of subbands, either when these latter are extremely correlated (first line with correlation coefficient $rho = 0.94$) or when they exhibit a small correlation (second line with correlation coefficient $rho = 0.44$).

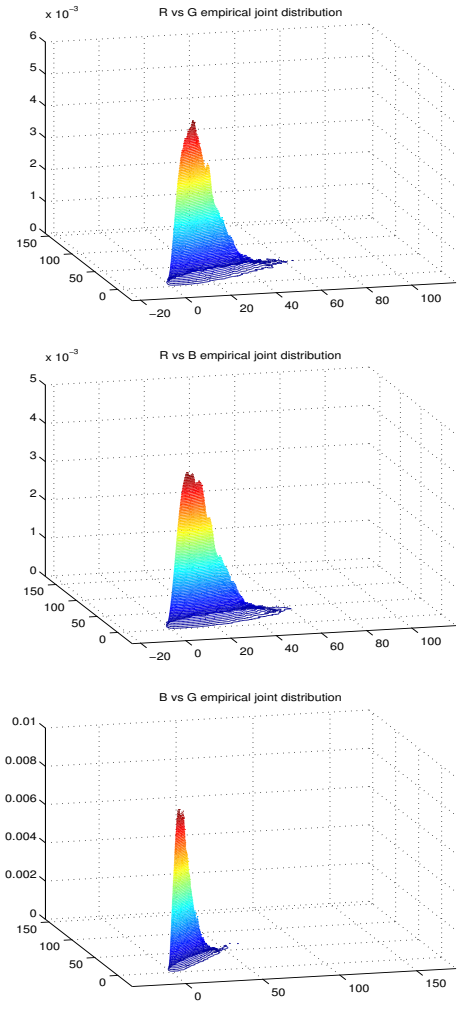

Fig. 9 Empirical joint distributions considering combinations of subbands of different color components.

3.4 Parameter estimation

For estimating parameters of MGΓD, we use the IFM (Inference From Margins) method [17]. Firstly, this consists in estimating the parameters of the marginals using the Maximum Likelihood procedure. Let $w_i = (\alpha_i, \tau_i, \lambda_i)$ be the parameters of the marginal f_i. ML estimators $\hat{w}_i$ are deduced as shown in Appendix A.

Secondly, the log-likelihood function for the joint distribution is minimized

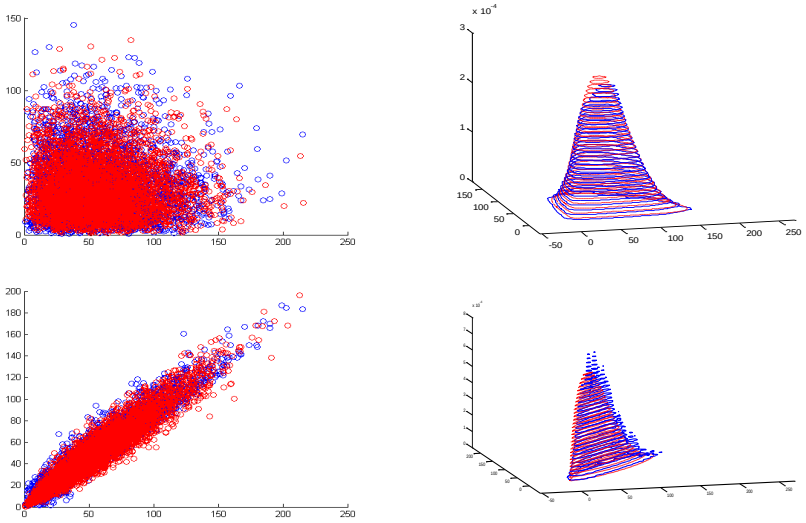

Fig. 10 Column of the left: fitting of samples generated from MGΓD model (red points) on original subband coefficients (blue points). Column of the right: fitting of the MGΓD density (red line) on coefficients joint empirical density (blue line)

using the estimated margins $\hat{w}$=($\hat{w}_1$, ..., $\hat{w}_d$):

$$\hat{\Sigma} = argmax_{\Sigma} \sum_{i=1}^{n} \log c(F_1(x_{1i}; \hat{w_1}), ..., F_d(x_{di}; \hat{w_d}); \Sigma) \tag{9}$$

In the case of Gaussian Copula, Σ can be estimated by the following matrix:

$$\hat{\Sigma} = \frac{1}{M} \sum_{i=1}^{M} \vartheta_i {\vartheta_i}^T \tag{10}$$

with $\vartheta_i = (\phi^{-1}(F_1(x_1)...\phi^{-1}(F_d(x_d))^T$. M represents the number of observations associated to multivariate vectors x_d.

3.5 Similarity measurement

As in the context of texture retrieval, texture classification reposes on a pertinent similarity measurement step, especially when opting for an instance-based type of classifiers.
Do and Vetterli [1] proposed the KL divergence as a similarity measure between parametric representations, when independence is supposed among transform coefficients. However, deriving the KL divergence in the case of copula based multivariate models is a challenging task. In [7] and [8], authors proposed a

Monte-carlo approximation of the KL divergence. But, this approach is computationally expensive and is not deterministic, since the KL divergence differs depending on the random number generation. An alternative approach was proposed in [31], by employing the bayesian CBIR maximum likelihood selection rule as a similarity measure. This significantly reduced the execution time in comparison with the Monte-carlo based similarity measurement. However, authors stressed that, even if the joint copula based approach leads to better retrieval rates using the ML selection rule, the marginal approach excels in terms of the computational time due to the simple closed form expressions of the KL divergence when the marginal-only approach is considered. Hence, merging the joint approach with a closed form expression of the KL divergence as a similarity measure will be a major advantage.

In this work, we aim to exploit the copulas properties to come up with a closed form of the KL divergence between two MGΓD models.

As it is known, the most attractive feature of the Copula approach is the separability between the marginal space and the dependence structure. From Sklar's theorem (subsection 3.1), we see that for continuous multivariate distribution functions, the margins and the dependence structure can be separated [21]. That is, we can analyze the dependence structure of multivariate distributions without studying the marginal distribution. Moreover, it was proved in [27], that given a Copula C and under increasing and continuous functions of the marginals, C remains invariant (see Appendix A). So, the independency between the marginals space and the Copula space allows us to use the Kullback Leibler divergence for measuring similarity between two Gaussian copula based models. If we consider $f(x;\theta_1)$ and $g(x;\theta_2)$ two joint pdfs that respectively model two datasets T_1 and T_2:

$$f(x;\theta_1) = c(F_1(x_1),...,F_d(x_d))\prod_{i=1}^{d} f_i(x_i) \tag{11}$$

and

$$g(x;\theta_2) = c(F_1(x_1),...,F_d(x_d))\prod_{i=1}^{d} g_i(x_i) \tag{12}$$

as the sum of the KL divergences between the marginals and the Gaussian dependence structure.

Where $\theta_1 = \{(w_1^{(1)},...,w_d^{(1)}), \Sigma_1\}$ and $\theta_2 = \{(w_1^{(2)},...,w_d^{(2)}), \Sigma_2\}$ are the hyperparameters of f and g respectively.

$$KL(f(x;\theta_1), g(x;\theta_2)) =$$

$$KL_{margins}(f(x;(w_1^{(1)},...,w_d^{(1)})), g(x;(w_1^{(2)},...,w_d^{(2)}))+$$

$$KL_{Gaussian}(f(x;\Sigma_1), g(x;\Sigma_2)) \tag{13}$$

This can also be proved mathematically, as shown in the recent work of Lasmar & al. [20]. That is,

$$KL(f(x;\theta_1), g(x;\theta_2)) = \sum_{i=1}^{d} KL(f_i(x_i; w_i^{(1)}), g_i(x_i; w_i^{(2)}))$$

$$+0.5(tr(\Sigma_2^{-1}\Sigma_1)) + log\frac{|\Sigma_2|}{|\Sigma_1|} - d) \tag{14}$$

So, using the KL between two univariate $G\Gamma$ pdfs [9][10] we deduce a closed form of KL divergence between two MGΓD models as:

$$KL(f(x;\theta_1), g(x;\theta_2)) = d(\log(\frac{\tau_1\lambda_2^{\alpha_2\tau_2}\Gamma(\alpha_2)}{\tau_2\lambda_1^{\alpha_2\tau_2}\Gamma(\alpha_1)})+$$

$$+(\frac{\lambda_1}{\lambda_2})^{\tau_1}\frac{\Gamma(\alpha_1+\frac{\tau_2}{\tau_1})}{\Gamma(\alpha_1)} + \frac{\psi(\alpha_1)}{\tau_1}(\alpha_1\tau_1 - \alpha_2\tau_2) - \alpha_1)$$

$$+0.5(tr(\Sigma_2^{-1}\Sigma_1)) + log\frac{|\Sigma_2|}{|\Sigma_1|} - d) \tag{15}$$

This presents a huge advantage in terms of lower computational complexity when compared with the Monte-Carlo based approach proposed in [20].

4 Experimental Results

To evaluate the effectiveness of the proposed model we adopt color texture classification as an application. Note that the proposed model can be used for segmentation issue also. Our purpose is not to evaluate the performance of classifiers, we aim at quantifying the performance of the pair model/similarity, i.e. MGΓD/KLD. Thus, we consider only one classifier. The K-nearest neighbor (KNN) was chosen among a variety of classifiers, since it is straightforward, widely used and well referenced in the literature [28]. KNN is a kind of instance-based classifier, where the main idea is that decision is achieved from K-nearest neighbors and letting to the majority vote decide the outcome of the class labeling. The decision is defined from a given similarity measure. For all of our experiments, we consider the DTCWT [6] which is an oriented complex decomposition. In addition to its directional analysis, shift invariance and low redundancy properties, the DTCWT was chosen for its reduced computational time. The two-scale DTCWT with a Q-shift (14,14)-tap filter which is used. For all color texture samples, every color band of each subimage was normalized by subtracting its mean and dividing by its standard deviation. We recall that the similarity measure is given by:

$$D(T_1, T_2) = \sum_{s=1}^{N_s} KL(f(x_s^{T_1}, \theta_1^s), f(x_s^{T_2}, \theta_2^s)) \tag{16}$$

4.1 Experiments versus data diversity

In order to conduct representative experiments, we use different databases and various configurations of the experimental protocol leading to a large view of the proposed model performance in comparison with other ones from the state of the art. Firstly, the conventional Vistex databases [1,3,5,7,20,25] are used and also the Outex database which is a more challenging color texture database, since the color and texture information are not easily distinguishable. Secondly, the experiments were conducted on two sizes of sample respectively 32×32 and 128×128. We consider the following scenarios:

- First scenario, i.e. DB1: 32×32 Vistex, addressing a set of 24 textured images of size 512×512 from the Vistex database [22], shown in Fig. 11. The protocol follows the work of [30] and [11]. Each image was divided into subimages of size 32×32 pixels.We consider 96 from the resulting 256 subimages as the training set, while the remaining 160 subimages are considered as the test set. This dataset is used in order to evaluate robustness of our model even if very local spatial structures are considered.
- Second scenario, i.e. DB2: 128×128 Vistex, addressing a set of 54 textured images of size 512×512 from the Vistex database, shown in Fig. 12. The protocol follows the work of [1]. Each image was divided into subimages of size 128×128 pixels. This dataset is available on the Outex web site [23] as test suit Contrib TC 00006. For each texture, subimages are considered to form a checkerboard. The white half of subimages is then considered as the training set and the black half is used as the testing set. Hence, the training procedure will account for non uniformity of the original images.
- Third scenario, i.e. DB3: 128×128 Outex, addressing a set of 68 textured images of size 746×538 from the Outex database, shown in Fig. 13. Each image was divided into 20 subimages of size 128×128 pixels. Training and testing sets are obtained as with DB2.

4.2 Quantitative evaluation of performance

For evaluating performance, we repose on two criteria namely the percentage of classification and the precision (or predictive positivity) [29] to quantify informative measures respectively the true positive rate and false positive rate. For each class of color textures, let TP be the number of true positives, i.e. subimages correctly classified. We consider the two measures:

- The percentage of classification is the proportion of textures which were well labeled by the classifier over the number of false negatives, noted FN. The false negative is the number of subimages being wrongly considered as not class members given a specific class of textures. The Percentage classification is given as follows:

$$Percentage = \frac{TP}{TP + FN} \times 100\%. \tag{17}$$

Fig. 11 24 texture classes from Vistex database

– The precision of a classifier is the proportion of textures which were well labeled by the classifier over the number of false positive, noted FP. The false positives is the number of subimages being wrongly classified as class members given a specific class of textures. The precision is given as follows:

$$Precision = \frac{TP}{TP + FP}. \tag{18}$$

For a given class, the system can achieve a percentage classification with a score of 100%, and a lower precision. This means that the classifier is good at labeling subimages of this class, but attributes other elements to this class while, in fact, they are not members of this latter.

	k=1	k=2	k=3	k=4	k=5	k=6
DB1	90.76	91.37	92.45	**93.64**	91.24	90.37
DB2	94.94	95.47	96.72	**97.22**	96.59	95.36
DB3	75.25	75.50	77.85	**82.64**	77.05	76.50

Table 3 Average percentage classification of the KNN classifier for different values of k on DB1, BD2 and DB3 using MGΓD.

Results in Table 3 indicate that better average percentage classification rates are achieved for k=4. Hence, for all the next results we fixe the value of k at 4 neighbors.

	MG$\mathit{\Gamma}$D	MWbl	MGam	MGGD	GGD
Tex1	56.25	61.25	55.75	53.75	51.25
Tex2	84.37	85.50	86.12	83.12	48.75
Tex3	96.87	87.34	77.34	85.62	76.87
Tex4	91.25	84.37	88.42	86.25	91.25
Tex5	88.75	88.25	87.37	74.37	78.12
Tex6	85.00	85.37	89.50	83.12	71.87
Tex7	93.75	89.37	89.62	81.87	54.37
Tex8	91.87	94.62	89.12	70.00	90.62
Tex9	100.00	87.12	97.34	70.00	58.75
Tex10	100.00	83.00	89.75	83.75	92.50
Tex11	95.62	89.12	97.50	66.25	89.37
Tex12	99.37	90.75	93.20	67.50	98.12
Tex13	95.62	94	96.26	93.75	76.25
Tex14	99.37	97.37	97.75	88.75	62.50
Tex15	77.50	87.50	88.12	61.25	70.00
Tex16	100.00	95.37	87.24	73.12	100.00
Tex17	99.37	89.75	96.28	88.12	97.50
Tex18	99.37	87.75	89.75	85.00	93.12
Tex19	99.37	94.00	95.85	95.00	93.75
Tex20	98.75	100.00	100.00	100.00	98.12
Tex21	100.00	96.87	90.87	86.87	69.37
Tex22	100.00	98.24	99.56	98.12	89.37
Tex23	100.00	98.37	99.37	99.37	91.25
Tex24	95	95.86	95.85	95.00	61.25
Average	**93.64**	**90.04**	**90.73**	**82.08**	**79.34**

Table 4 Percentage classification of the KNN classifier for the MG$\mathit{\Gamma}$D, MWbl, MGam and MGGD models for 24 color textures (DB1).

4.3 Average classification rates for the MG$\mathit{\Gamma}$D model over other existing models

The first issue discussed in this experiment is to provide an experimental evidence of the flexibility and genericity of the proposed model over existing joint parametric models including the copula based Multivariate Gamma density proposed by **Stitou et al.** [25], the copula based Multivariate Weibull proposed by **Kwitt et al.** [7], and the Multivariate Generalized Gaussian density proposed by **Verdoolaege et al.** [5]. We also compare the proposed approach with the marginal modeling approach proposed by **Do et al.** [1] which assume independence between the color components. Let us give descriptions of these approaches:

- **Stitou et al.** : In this approach [25], authors proposed a Gamma based marginal modeling in conjunction with a Gaussian copula in order to characterize the local structure of wavelet subbands. We call this model, the Multivariate Gamma density *(MGam)*. L1 distance was used as similarity measure for this model, however, we will use the KL divergence as a similarity measure between MGam features in order to have a comparative look of the models (MG$\mathit{\Gamma}$D vs MGam). For this, we use the expression of

KL divergence between Gamma densities [3] and the KL divergence of the Gaussian copula (Equation (13)).

- **Kwitt et al.**: In [7], Kwitt et al. proposed a student t copula based multivariate Weibull *(MWbl)* model for characterizing magnitudes of complex subbands coefficients, besides cross color components dependency. As we already mentioned (subsection 3.5), a computationally expensive Monte-Carlo based approach was adopted to overcome the lack of closed-form of the KL divergence. In [31], authors employed the ML selection rule of the Content Based Image Retrieval (CBIR) framework as an alternative of the Monte-carlo based approach, but without providing a closed-form expression of the KL divergence. Here we use our approach for measuring KL divergence between MWbl models (Equation (13)), in order to compare performances of the MGΓD and MWbl models.
- **Verdoolaege et al.**: In [5], Verdoolaege et al. proposed the Multivariate Generalized Gaussian (MGGD) model for color texture retrieval. Authors overcome the lack of closed-form expression of the KL divergence by proposing a closed-form expression of the geodesic distance. Verdoolaege et al. modeled dependency across subbands of the R,G and B color components while assuming independence between subbands of the same color component. We use the same parametrization in our experiment, in order to compare our approach to Verdoolaege et al. approach, in terms of the model (MGΓD vs MGGD), the similarity measure (KL divergence vs Geodesic distance) and in term of the modeled dataset since we consider non-Zero dependence across subbands of a given color component.
- **Do et al.**: The marginal modeling approach proposed by Do & Vetterli [1], has shown efficiency of the Generalized Gaussian density (GGD) in the case of grey level texture retrieval. For color textures characterization, the marginal approach consists in modeling each of the color components independently using GGD model and then concatenate the features in one global vector.

Table 4 and Table 5 show respectively the percentage classification and the precision of the KNN classifier for all 24 textures of DB1. We firstly remark the large gain of performances of the multivariate approach over the marginal GGD based approach. This approves our dependence observations in the RGB color space, and shows the huge loss of information when the correlation between color components is omitted.

The second main observation that can be deduced from Table 4 and Table 5, is the flexibility of the MGΓD over the MWbl and MGam models which can be considered as special cases of MGΓD. Our model gives better performances in term percentage and precision of the classification. This behavior remains the same for most of the 24 color textures of DB1, and is due to the genericity of the characterization that offers MGΓD reposing on its additional shape parameter.

In Table 6 and Table 7, we show the average percentage classification and the average precision for DB1, DB2 and DB3. For all these databases, our

Fig. 12 54 texture classes from Vistex database.

Fig. 13 68 texture classes from Outex database.

model achieves the best results, even we remark the hardiness of classifying in the Outex Database (DB2), which is due, as we said above, to the diffi-

	MGΓD	MWbl	MGam	MGGD	GGD
Tex1	1.00	0.97	0.95	0.94	0.98
Tex2	0.83	0.73	0.81	0.80	0.39
Tex3	1.00	1.00	1.00	0.89	1.00
Tex4	0.99	0.95	0.80	0.97	0.95
Tex5	1.00	0.98	0.83	0.82	0.87
Tex6	0.94	0.83	0.93	0.90	0.76
Tex7	0.81	0.78	0.82	0.90	0.54
Tex8	0.98	0.99	0.98	0.67	0.93
Tex9	0.96	0.98	0.96	0.81	0.68
Tex10	0.98	1.00	0.98	0.89	0.81
Tex11	0.88	0.83	0.86	0.81	0.61
Tex12	1.00	0.98	0.94	0.83	0.98
Tex13	0.95	0.88	0.90	0.64	0.80
Tex14	0.85	0.84	0.81	0.89	0.71
Tex15	0.97	0.73	0.95	0.58	0.78
Tex16	1.00	1.00	1.00	0.45	0.93
Tex17	0.75	0.80	0.76	0.62	0.70
Tex18	0.89	0.95	0.90	0.74	0.90
Tex19	0.92	0.98	0.91	0.97	0.89
Tex20	0.90	0.92	0.90	0.95	0.76
Tex21	0.88	0.86	0.87	0.90	0.72
Tex22	1.00	1.00	1.00	0.86	0.71
Tex23	0.97	0.93	0.98	0.93	0.84
Tex24	0.91	0.75	0.88	0.99	0.79
Average	0.93	0.90	0.90	0.82	0.79

Table 5 Precision of the KNN classifier for the MGΓD, Mwbl, Mgam and MGGD models for 24 color textures (DB1).

	MGΓD	MWbl	MGam	MGGD	GGD
DB1	93.64	90.04	90.73	82.08	79.34
DB2	97.22	95.45	95.80	89.75	84.12
DB3	82.64	77.3	78.61	73.64	70.37

Table 6 Average classification rate for three scenarios.

	MGΓD	MWbl	MGam	MGGD	GGD
DB1	0.93	0.90	0.90	0.82	0.79
DB2	0.98	0.95	0.96	0.90	0.87
DB3	0.85	0.80	0.82	0.80	0.78

Table 7 Average precision for three scenarios.

	MGΓD	MWbl	CopGGD
Proposed KLD	97.22	95.45	94.50
Monte-Carlo KLD	96.45	94.70	94.37

Table 8 Average classification rate for different models using Monte-Carlo based KLD and the proposed KLD.

	Proposed approach	Monte-Carlo
DB1	94.95	1.21×10^3
DB2	4.9	60
DB3	2.03	25.63

Table 9 Execution time (in minutes) for calculating similarity measure matrix between the learning and testing set for DB1, DB2 and DB3 using MGΓD model

culty of distinguishing color and texture information in this database. We, also, clearly observe that our approach achieves higher rates in comparison with the MGGD presented in [5]. This approves our consideration of non-Zero dependence across same color component subbands (see Fig. 3) since we consider inter-component and inter-band dependencies.

The second issue to be discussed is the similarity measure. We compare the proposed KL divergence with the Monte-Carlo based approach [7][8]. In [8], Sakji-Nsibi et al. used the Monte-carlo based KL divergence, as a similarity measure between generalized Gaussian copula based GGD (*CopGGD*) feature representations. Table 8, presents average percentage classification using both similarity measure approaches for the MGΓD, MWbl and CopGGD models, i.e. parametric closed form and Monte-Carlo method. The proposed similarity measure slightly outperforms the Monte-Carlo based approach in term of percentage classification. However, the improvement is more significative in term of execution time as can be clearly seen from Table 9. The computational time can be estimated as 12 times less when using our approach for measuring similarity between copula-based joint models. We note that the experiments were done using Matlab environment on an HP Compaq dc 5800SFF, equipped with an Intel Core 2 Duo CPU at 3GHZ and 1GB of RAM, with a 32-bit Windows vista operating system.

5 Conclusion

We have proposed a joint generic model for characterizing DTCWT coefficient magnitudes of color textures. MGΓD presents a pertinent color texture description in comparison with the marginal approach that assumes independence among color component subbands. MGΓD, also presents a flexible modeling when compared with variety of joint models. We, further, proposed a simple, faster and closed form expression similarity measure using the independence between the marginals space and the dependence structure. The genericity of the proposed model and the pertinence of the similarity measure allowed us to achieve good improvement in terms of classification rate and computational time.

In future works we would like to use copulas for characterizing color textures in luminance-chrominance color spaces such as L*a*b* or HSV. In such color spaces, the separation between luminance and chrominance information need to a multi-model characterization in order to improve classification rates.

A

Supposing $y = (y_1, y_2, ..., y_M)$, a set of M independent coefficients, The maximum likelihood function of the sample is defined as:

$$y : L = \log \prod_{i=1}^{M} f(y; \alpha, \tau, \lambda) \tag{19}$$

$$\frac{\partial L}{\partial \alpha} = -M(\tau \log \lambda - \psi(\alpha)) + \sum_{i=1}^{M} \tau \log y_i = 0. \tag{20}$$

$$\frac{\partial L}{\partial \tau} = M(\frac{1}{\tau} - \alpha \log \lambda) +$$

$$\sum_{i=1}^{M} \alpha \log y_i - (\frac{y_i}{\lambda})^{\tau} \log \frac{y_i}{\lambda} = 0. \tag{21}$$

$$\frac{\partial L(y; \alpha, \tau, \lambda)}{\partial \lambda} = -\frac{M\alpha\tau}{\lambda} + \frac{\tau\lambda^{-\tau}}{\lambda} \sum_{i=1}^{M} y_i = 0. \tag{22}$$

Thus, the parameters are deduced by solving a system of three equations:

$$\hat{\lambda} = [\frac{1}{M\hat{\alpha}} \sum_{i=1}^{M} {y_i}^{\hat{\tau}}]^{\frac{1}{\hat{\tau}}}. \tag{23}$$

$$\hat{\alpha} = \frac{1}{\hat{\tau}} [\frac{\sum_{i=1}^{M} {y_i}^{\hat{\tau}} \log y_i}{\sum_{i=1}^{M} {y_i}^{\hat{\tau}}} - \log y_i]^{-1}. \tag{24}$$

$$\log \frac{M\hat{\alpha}(\prod_{i=1}^{M} y_i)^{\frac{\hat{\tau}}{M}}}{\sum_{i=1}^{M} {y_i}^{\hat{\tau}}} - \psi(\hat{\alpha}) = 0. \tag{25}$$

where ψ denotes the digamma function. In [9], we tackled the high nonlinearity of the ML equations by using a numerical approximation based on the algorithm of Cohen et al. [13]. However, a faster algorithm was proposed in [10], in which a Scale-Independent Shape Estimation (SISE) method is used to find roots of the ML equations.

B

The proposition presented in [27], shows one attractive feature of the Copula representation of dependence, namely that the dependence structure when modeled by a Copula is invariant under increasing and continuous transformations of the marginals.

If $(x_1, ..., x_n)^t$ has copula C and $T_1, ..., T_n$ are increasing continuous functions, then $(T_1(x_1), ..., T_n(x_n))^t$ also has copula C.

References

1. M. Do and M. Vetterli, "Wavelet-based texture retrieval using generalized Gaussian density and Kullback-Leibler distance," *IEEE transactions on image processing*, vol. 11, pp. 146–158, 2002.
2. J. Mathiassen, A. Skavhaug, and K. Bø, "Texture Similarity Measure Using Kullback-Leibler Divergence between Gamma Distributions," in *European Conference on Computer Vision 2002*, 2002, pp. 19-49.
3. R. Kwitt and A. Uhl, "Image similarity measurement by Kullback-Leibler divergences between complex wavelet subband statistics for texture retrieval," in *Image Processing, 2008. ICIP 2008. 15th IEEE International Conference*, 2008, pp. 933-936.
4. G. Tzagkarakis, B. Beferull-Lozano, and P. Tsakalides, "Rotation-invariant texture retrieval with gaussianized steerable pyramids," *IEEE transactions on image processing*, vol. 15, pp. 2702-2718, 2006.
5. G. Verdoolaege, S. De Backer, and P.Scheunders, "Multiscale colour texture retrieval using the geodesic distance between multivariate Generalized Gaussian models," in *Proceedings of the 15th IEEE Interational Conference n Image Processing (ICIP'08)*, 2008, pp. 169–172.
6. N. Kingsbury, *"The Dual-Tree Complex Wavelet Transform: A new Technique for Shift-Invariance and Directional Filters,"* in Proceedings of the 8th IEEE DSP Workshop, Aug. 1998, pp. 9-12.
7. R. Kwitt and A. Uhl, "A joint model of complex wavelet coefficients for texture retrieval," in *Image Processing, 2009. ICIP 2009. 16th IEEE International Conference*, 2009, pp. 1877-1880.
8. S. Sakji-Nsibi and A. Benazza-Benyahia, "Fast scalable retrieval of multispectral images with kullback-leibler divergence,textquotedblright in *Image Processing, 2010. ICIP 2010. 17th IEEE International Conference*, 2010, pp. 2333-2336.
9. A. D. EL Maliani, M. EL Hassouni, N. Lasmar and Y. Berthoumieu, "Texture classification based on the Generalized Gamma distribution and the Dual Tree Complex Wavelet Transform," in *5th International Symposium on I/V Communications and Mobile Network (ISIVC)*, 2010, pp. 1-4.
10. S. K. Choy and C.S G.Tong, "Statistical Wavelet Subband Characterization Based on Generalized Gamma Density and Its Application in Texture Retrieval," *IEEE transactions on image processing*, vol. 19, pp. 281 - 289, 2010.
11. I. Qazi, O. Alata, J.C. Burie and C.F. Maloigne "Color spectral analysis for spatial structure characterization of textures in IHLS color space," *Pattern Recognition*, vol. 43, pp. 663–675, 2010.
12. Ye Mei and D. Androutsos, "Color texture retrieval using wavelet decomposition in the independent components color space," in *Canadian Conference on Electrical and Computer Engineering. CCECE 2008.* , 2008, pp. 001379 - 001382.
13. A. C. Cohen and B.J. Whitten, *Parameter Estimation in Reliability and Life Span Models*. Marcel Dekker, 1988.
14. Kai-Sheng Song, "Globally Convergent Algorithms for Estimating Generalized Gamma Distributions in Fast Signal and Image Processing," *IEEE transactions on image processing*, vol. 17, pp. 1233-1250, 2008.
15. R. B. Nelsen, *An Introduction to Copulas*. Springer Series in Statistics. Springer, second edition, 2006.
16. M. Sklar, "Fonctions de répartition à n dimensions et leurs marges,". *Publications de l'institut de Statistique de l'Université de Paris*. vol. 8, pp. 229-231, 1959.
17. H. Joe, *Multivariate Models and Dependence Concepts*. Monographs on Statistics and Applied Probability. Chapman & Hall, 1997.
18. E. W. Stacy, "A Generalization of the Gamma Distribution,". *Ann. Math. Statist.* vol. 33, pp. 1187-1192, 1962.
19. G. Van De Wouwer , P. Scheunders and D. Van Dyck, "Statistical Texture Characterization From Discrete Wavelet Representations," *IEEE transactions on image processing*, vol. 8, pp. 592 - 598, 1999.
20. N. Lasmar, Y. Berthoumieu, "Gaussian Copula Multivariate Modeling for Image Texture Retrieval Using Wavelet Transforms," *submitted to IEEE transactions on image processing*.

21. M. Bohdalova, and O. Nanasiova, "A note to Copula Functions," *E-leader Bratislava*, vol. 11, pp. 15, 2006.
22. "MIT vision and modeling group," [Online], Available from: http://vismod.media.mit.edu.
23. "http://www.outex.oulu.fi/,".
24. T. Ojala, T. Maenpaa, M. Pietikainen, J. Viertola, J. Kyllonen, and S. Huovinen, "Outex - new framework for empirical evaluation of texture analysis algorithms," in *In Proceedings of 16th International Conference on Pattern Recognition*, 2002, pp. 10701.
25. Y. Stitou, Y. Berthoumieu and N. Lasmar, "Copulas based multivariate gamma modeling for texture classification," in *icassp, IEEE International Conference on Acoustics, Speech and Signal Processing 2009*, Taipei, Taiwan, April 19-24, 2009, pp. 1045-1048.
26. N. Fisher and P. Switzer, "Chi-plots for assessing dependence," *Biometrika.* vol. 72, pp. 253-265, 1985.
27. P. Embrechts, A. McNeil, and D. Straumann, *Correlation And Dependence In Risk Management: Properties And Pitfalls, RISK MANAGEMENT: VALUE AT RISK AND BEYOND.* Cambridge University Press, 1999, pp. 176-223.
28. T. M. Cover and P. E.Hart, "Nearest neighbor pattern classification," *IEEE Trans. Inform. Theory*, vol. 13, pp. 21-27, 1967.
29. B. Dorizzi R. V. Andreao and J. Boudy, "ECG signal analysis through hidden Markov models," *IEEE Transactions on Biomedical Engineering*, vol. 53(8), pp. 1541-1549, 2006.
30. H. Permuter, J. Francos, and I. Jermyn, "A study of gaussian mixture models of color and texture features for image classification and segmentation," *Pattern Recognition*, vol. 39(4), pp. 695-706, 2006.
31. R. Kwitt, P. Meerwald and A. Uhl, "Efficient Texture Image Retrieval Using Copulas in a Bayesian Framework," *IEEE transactions on image processing*, vol. 20, pp. 2063-2077, 2010.
32. C. Genest and A. C. Favre, "Everything you always wanted to know about Copula modeling and were afraid to ask," *Journal of Hydrological Engineering*, vol. 12, pp. 347-368, 2007.